11th Edition of the

International Conferences on
Wind Turbine Noise

Copenhagen, Denmark – 10th to 13th June 2025

Turbulent boundary layer trailing-edge noise reduction with permeable blade extensions at full-scale conditions

Friso H. Hartog[1], Tjeu A. Gehlen, and Michiel van Nesselrooij
MuTech B.V., Delft, 2629 HS, The Netherlands

Summary

Serrations are the current industry standard for reducing turbulent-boundary-layer trailing-edge noise, which is typically the main noise source for wind turbine rotor blades. Unfortunately, these well-known devices have little room for improvement, putting the growth of onshore wind energy need to reach climate and energy independence goals at risk. This accentuates the need for next-generation technologies for broadband noise reduction such as permeable trailing-edge extensions.

The present work covers wind tunnel experiments conducted in the Poul la Cour Tunnel (PLCT) at the Technical University of Denmark (DTU). Different designs for permeable blade extensions were produced using additive manufacturing, measured on a 900 mm FFA W3-211 airfoil model using an 84-microphone array, and compared against reference serrations. Results show improved performance at typical operating conditions (α = 8°, U_∞ = 80 m/s), with maximum reductions of 15 dB in sound pressure level (SPL) and 8 dB(A) in A-weighted overall sound pressure level (O(A)SPL) compared to an untreated blade, and up to 3 dB(A) improvement in O(A)SPL over serrations. Furthermore, unified empirical length scaling laws are introduced that address different aeroacoustic mechanisms. This enables tailored designs for different blade geometries and operational regimes to maximise overall noise reduction.

These findings represent a significant step toward translating permeable trailing-edge extensions from laboratory concepts into commercially viable solutions. With demonstrated robust acoustic performance at full scale, permeable extensions offer a highly promising path forward for reducing wind turbine noise and supporting the broader deployment of onshore wind.

1. Introduction

Wind turbine noise presents a multifaceted impact: it contributes to environmental pollution and restricts the growth of onshore wind energy, putting climate goals and energy independence needs at risk. Among the various noise sources, turbulent boundary-layer trailing-edge (TBL-TE) noise dominates for modern, large-scale wind turbines [1]. Trailing-edge serrations have become the industry standard for mitigating this noise [2–4], but their potential for further optimization is limited. To unlock further noise reductions that enable broader public acceptance and further the adoption of onshore wind, new approaches are needed. Permeable trailing-edge extensions have emerged as a promising candidate for next-generation noise abatement.

[1]Corresponding author - Email: f.hartog@muteskin.eu

Research in the past decade has demonstrated that permeable trailing edges can significantly reduce TBL-TE noise [5–16]. Various implementations, ranging from metal foam inserts [5–8, 12] to perforated add-ons [9–11, 13–15], have shown promising results in experiments and high-fidelity simulations. They can achieve broadband noise reductions of over 10 dB at low-to-moderate frequencies when properly designed [10, 11, 13, 14]. This reduction has been attributed to several mechanisms, such as the pressure release process [8, 12, 13, 15], breaking of turbulence coherence [15], and distributed scattering [12, 13, 15]. A secondary, mild noise-increasing effect occurs at higher frequencies due to the introduced surface roughness [8, 15]. Additionally, for certain designs, pore-induced vortex shedding can generate extra quasi-tonal peaks [15, 16]. The net result of these three effects typically ranges from 4 to 6 dB reduction in overall sound pressure levels (OSPL) at low Reynolds numbers [10, 11].

Despite promising results at scaled conditions, a critical gap remains in translating this technology to industrial applications. To our knowledge, no full-scale data is available in the literature, and key practical aspects — such as aerodynamic performance, manufacturability, and durability — remain largely unaddressed. These unknowns are further compounded by the vast design space and the resulting challenges in scaling to operational conditions of wind turbine rotor blades. As a result, a technology with clear promise was at risk of remaining "in the lab", unable to contribute meaningfully to the much needed expansion of wind energy.

This work aims to move permeable blade extensions closer to becoming a viable technology for wind turbine noise reduction. We present the first publically available, full-scale acoustic results of permeable blade extensions, measured in the Poul la Cour Tunnel (PLCT). These add-ons achieve an additional 3 dB(A) reduction in overall noise levels compared to serrations and can be manufactured and applied using industry-standard methods and materials. We also introduce scaling laws that enable design tailoring to different blade geometries and operational conditions. Proprietary constraints limit data disclosure; however, key findings and trends are shared to highlight the important advancements in this area.

2. Methodology

The present work covers an experimental wind tunnel campaign at full-scale conditions, measuring rotor blade trailing-edge noise with different noise-reducing trailing-edge devices. The wind tunnel and test section are described in Section 2.1, followed by more details on the models and conditions in Section 2.2, and an explanation of the data acquisition and processing procedure in Section 2.3. Given the use of established, standardized procedures — common for commercial testing at this facility — method descriptions are kept concise. Where relevant, references to more detailed documentation are provided.

2.1 Wind tunnel and test section

Tests were performed in the Poul la Cour Tunnel (PLCT), on the Risø Campus of the Technical University of Denmark (DTU) in Roskilde, Denmark. It is a state-of-the-art facility dedicated to aerodynamic and (aero)acoustic measurements for wind turbine applications, in particular rotor blade sections. The wind tunnel operates as a closed-loop system powered by a 2.4 MW fan to reach maximum flow speeds of up to 105 m/s. The test section measures 2 m × 3 m × 9 m (H × W × L) and has interchangeable sidewalls, which are solid and tensioned Kevlar in the aerodynamic and acoustic configurations, respectively. The test section is contained within a larger, acoustically treated anechoic room, while the rest of the system also contains acoustic aborbent treatments. This allows for acoustic measurements that approach ideal free-field conditions. For the present study, the acoustic configuration was used. More details on the facility can be found in Ref. [17].

2.2 Models and conditions

2.2.1 Blade model

A 900mm chord FFA W3-211 [18] airfoil model was used, with a 0.4 mm ZZ-trip at 5% and 10% x/c on the suction side and pressure side, respectively. The set geometric angle of attack α_{geom} was translated into an effective angle of attack α_{eff} by matching the pressure distribution curves as measured in the wind tunnel and simulated with XFOIL [19], following the procedure outlined in [11]. The airfoil and $\alpha-$matching curve are shown in Figure 1. The global fit agrees well with the matching of individual cases and provides confidence in the accuracy of the estimated α_{eff}, which is used as α from hereon in presenting and discussing the results.

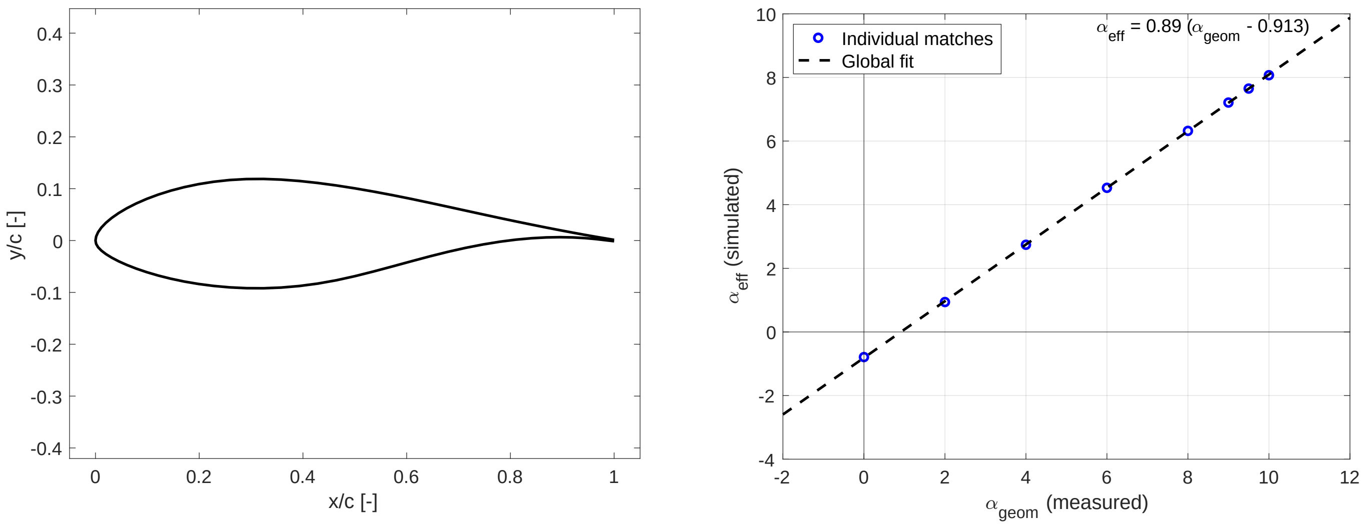

(a) (b)

Figure 1 Blade model setup. (a) FFA W3-211 cross-sectional shape. (b) Translation of geometric to effective angle of attack.

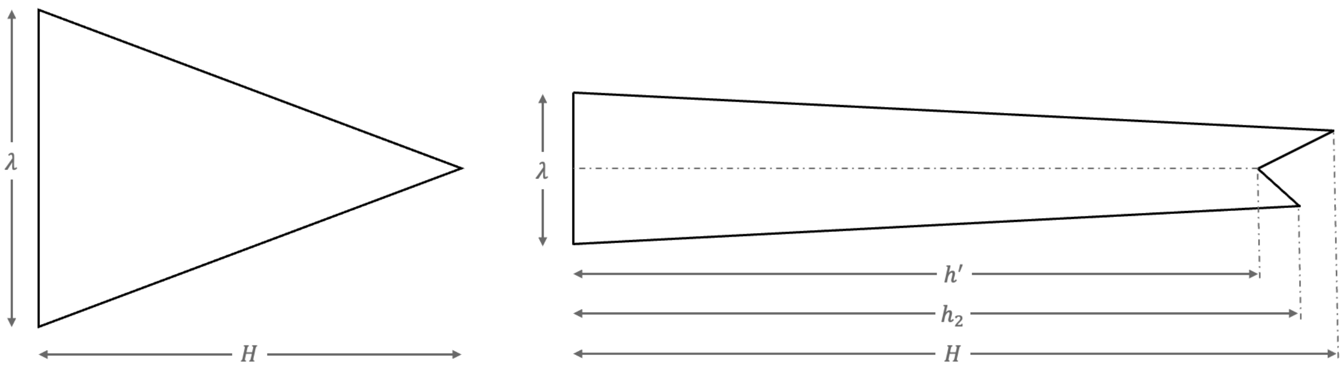

Parameter	H	λ
Value [mm]	100	75

Parameter	H	λ	h'	h_2
Value [mm]	180	36	162	172

Figure 2 Reference serrations: conventional sawtooth (left) and double-rooted (right).

2.2.2 Trailing-edge models

Two serrated add-on models were selected as references for known noise-reducing technologies. The first model has a conventional sawtooth serrated geometry and is made of industrial-grade material. The second model has a double-rooted geometry and is based on input provided by Brunel University - see Ref. [20] for their work. These two models were selected to represent the status quo (former model) and a potential evolution (latter model) in serrations. Their planforms are visualised in Figure 2, and they are hereafter referred to as serrations and double-rooted trailing-edge serrations (DRooTES), respectively.

The permeable blade extension models covered variations in key design parameters, such as extension length (l_{ext}) and flap angle (β). While the focus of this study is on acoustic performance, aerodynamic considerations were taken into account during the design process. Previous campaigns have shown that well-designed permeable extensions have a limited influence on lift, drag, and stall behaviour, with β being the dominant governing parameter. By tuning β, load-neutral behavior — defined as 0% change in lift at a target design α — was achieved within 0.5° of the predicted neutral-load β. Notably, this condition typically aligns closely with β that yields optimal noise reduction, forming a natural design point for the presented results. Minor increases in drag (typically under 10%) can be compensated by small, controlled increases in lift of approximately 2%, maintaining overall aerodynamic efficiency. All add-ons in this study were designed with this balance of acoustics and aerodynamics in mind, ensuring that the optimised acoustic results reported are representative of aerodynamically viable configurations.

The add-ons measured in this campaign were produced using additive manufacturing methods to allow for many design variations and extensive parameter sweeps in testing. In addition, the most challenging design from a manufacturing perspective was successfully produced using injection moulding with standard materials commonly applied in add-ons such as vortex generators and serrations. This trial production demonstrated the feasibility of manufacturing permeable add-ons using industry-accepted methods and materials. Specific geometric details and parameter values are omitted due to confidentiality requirements.

2.2.3 Test conditions

Measurements were conducted at a range of angles of attack and flow velocities typical for operating conditions. For some designs, more resolution was provided in the angles of attack and/or velocities to collect additional data for scaling purposes. Also, for some designs, the case of natural transition was measured. Lastly, the constraints in the available testing time required abbreviated testing and hence a limited number of conditions for some models. A summary is provided in Table 1.

Table 1 Test conditions for different cases. Some permutations (e.g. joint high resolution sweeps of α and U_∞) are not explicitly included.

Test cases	α_{geom} [°]	U_∞ [m/s]	$Re_{c,max}$ [−]	Transition [-]
All	-4, 0, 4, 6, 8, 10, 11	55, 70, 85	5.5×10^6	Forced
Some	-8:2:6, 7:1:11	55, 70, 85	5.5×10^6	Forced
Some	-4, 0, 4, 6, 8, 10, 11	55, 70, 75, 80, 85	5.5×10^6	Forced
Some	-4, 0, 4, 6, 8, 10, 11	55, 70, 85	5.5×10^6	Natural

2.3 Data acquisition and processing

Acoustic measurement data was collected with an 84-channel microphone array located in the anechoic room outside the test section at a 2.3 m distance from the blade trailing-edge. Acoustic source maps were computed with conventional frequency-domain beamforming, an example of which is shown in Figure 3a. Subsequent source levels were obtained from the depicted integration window in the form of span-normalised spectra as shown in Figure 3b. Overall levels are calculated within the 200 – 5000 Hz domain. More details on the post-processing procedure can be found in Ref. [21].

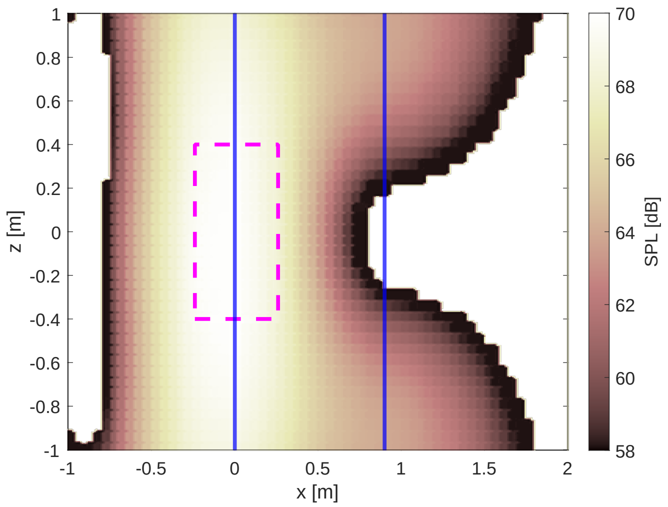

(a)

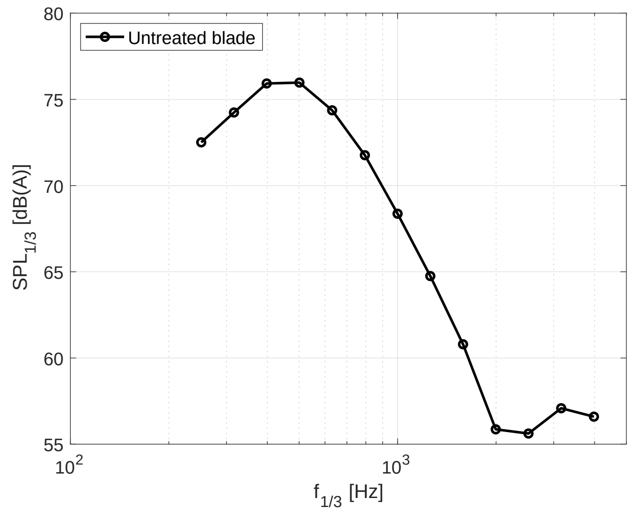

(b)

Figure 3 Beamforming results for untreated case at $U_\infty = 80\,\mathrm{m/s}$, $\alpha = 8°$. (a) Source map at $f_{1/12} = 527\,\mathrm{Hz}$. Flow from right to left. Blue indicates airfoil LE and TE, magenta indicates integration window. (b) Integrated spectrum.

3. Results and discussion

This section presents the key acoustic results from the wind tunnel campaign. General acoustic performance for a specific permeable blade extension design is compared to that of the reference serrations in Section 3.1. Subsequently, Section 3.2 discusses the abatement of quasi-tonal humps for particular designs of permeable extensions. Lastly, Section 3.3 presents relevant scaling laws for permeable extensions.

3.1 General acoustic performance

The acoustic performance of the tested add-ons is evaluated relative to the untreated blade to quantify their noise reduction capacity. Figure 4a presents the difference in sound pressure level (ΔSPL) at the target design condition of $U_\infty = 80$ m/s and $\alpha = 8°$, comparing the serrations, DRooTES, and permeable extension. While both the serrations and DRooTES achieve a maximum reduction of around 7 dB, the permeable extension delivers a significantly larger reduction, reaching up to 14 dB. The stronger reduction compared to scaled tests reported in the literature suggests that permeable trailing-edge extensions benefit from scaling effects, which increase their effectiveness as blade chord, flow velocity, and absolute noise levels increase. Additionally, this superior performance spans a broad frequency range from approximately 250-300 Hz up to 1,500-2,000 Hz, effectively covering the frequencies of primary relevance for wind turbine noise emission.

The robust performance of the permeable extension across varying α is illustrated in Figure 4b. The magnitude, center frequency, and width of the noise reduction region ('bucket') remain relatively stable with α. At higher frequencies, a slight increase in noise is observed, attributable to surface roughness effects. The cross-over frequency at which this occurs shows a subtle dependence on α, especially between 5° and 10°, where aerodynamic loading effects become more pronounced. This spectral behaviour of the permeable extension highlights its strong potential for operational wind turbine applications. First, its robustness to variations in α ensures effective noise reduction across the full range of operating wind speeds and radial positions along the blade. Second, the dominance of noise reduction at low-to-medium frequencies aligns favourably with real-world conditions, where atmospheric absorption disproportionately attenuates higher frequencies before reaching ground-level observers.

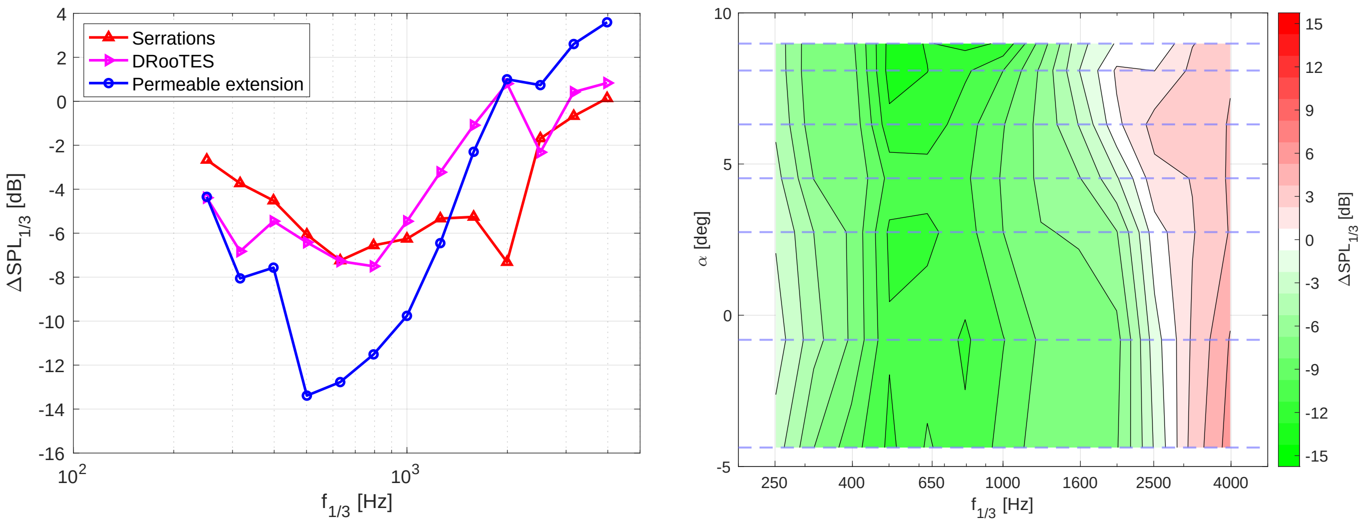

(a) (b)

Figure 4 Difference in sound pressure level compared to an untreated blade at $U_\infty = 80$ m/s. (a) Different devices at $\alpha = 8°$. (b) Permeable extension at different α. Blue lines indicate α with available data, between which values are interpolated to generate the map.

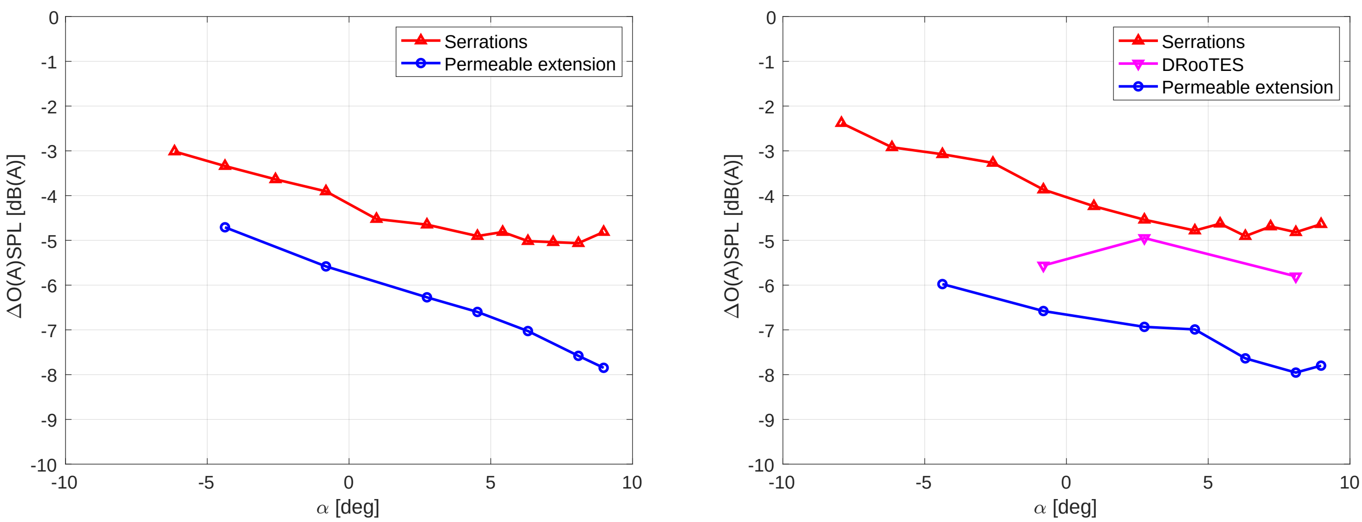

(a) (b)

Figure 5 Difference in overall A-weighted sound pressure level compared to an untreated blade. (a) $U_\infty = 70$ m/s (b) $U_\infty = 80$ m/s.

The improved performance of the permeable extension across the key frequency range also translates into a significantly lower overall sound pressure level (OSPL). Figure 5 presents the results at 70 m/s and 80 m/s. Testing at full-scale conditions warrants the use of A-weighted levels, in line with the IEC standard for field measurements [22]. Compared to the DRooTES and serrations, the permeable extension achieves an additional reduction in O(A)SPL of up to 2–3 dB(A), with relatively stable performance across the range of α. This improvement results in a maximum overall noise reduction of 8 dB(A) at the target design condition, representing a substantial step in performance over the state-of-the-art.

3.2 Abatement of quasi-tonal humps

Flow over permeable trailing-edge extensions can induce local vortex shedding, leading to the generation of tonal peaks in the acoustic spectrum [15, 16]. This phenomenon is expected to become more pronounced at larger scales, due to increased flow velocity and blade chord length. Figure 6 shows that for certain designs, quasi-tonal humps appear as localized discontinuities within the broadband noise reduction bucket. These features were found to scale with velocity in accordance with a Strouhal-type relationship, suggesting an aeroacoustic origin such as vortex shedding at different characteristic length scales.

Targeted design modifications were implemented to suppress these tonal features without compromising the broadband noise reduction performance, which is particularly clear at the lowest frequencies where the spectra remain identical. The successful mitigation of these local effects was achieved consistently across different extension geometries, indicating that the underlying physical phenomenon can be effectively controlled through appropriate design strategies, regardless of the specific extension configuration.

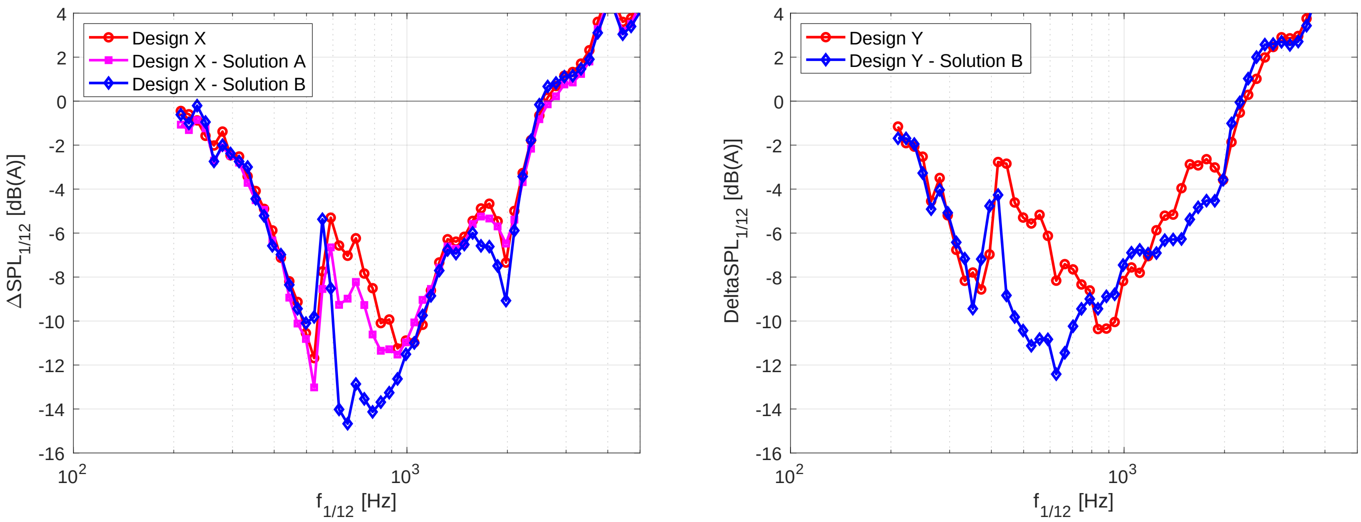

Figure 6 Difference in sound pressure level compared to an untreated blade at $U_\infty = 80$ m/s and $\alpha = 2.7°$. (a) Baseline design X. (b) Baseline design Y.

3.3 Extension length scaling

To demonstrate the ability to tailor permeable extension designs to different blade geometries and operational conditions, we introduce scaling laws for a key design parameter: the extension length, l_{ext}. Figure 7a shows the unscaled noise reduction curves for five different extension lengths. Not all lengths included targeted modifications to suppress quasi-tonal humps. Therefore, for the purpose of this analysis, the spectra were corrected to omit these humps, similar to the demonstrated effects of such modifications as discussed in Section 3.2.

The data show a clear trend: longer extensions perform better at lower frequencies, while shorter extensions provide greater noise reduction at higher frequencies. However, the dependence on l_{ext} differs in magnitude between the two frequency regimes, as illustrated in Figures 7b and 7c. In the lower frequency range, noise reduction curves collapse when the frequency is scaled linearly with l_{ext}, consistent with a Strouhal-type scaling typical of TBL-TE noise. In contrast, the higher frequency range collapses when scaled with $l_{ext}^{1/2}$. This corresponds to the roughness-induced noise increase mechanism, which can be shown — see Equations (1) and (2) — to follow an approximate square-root dependence of f on l_{ext} based on Amiet's theory [23] and a change in displacement thickness (δ^*) due to the add-on [24]. The distinct empirical scaling laws — linear with l_{ext} at lower frequencies and proportional to $l_{ext}^{1/2}$ at higher frequencies — explain why longer extensions achieve broader noise reduction across a wider range of turbulent eddy scales.

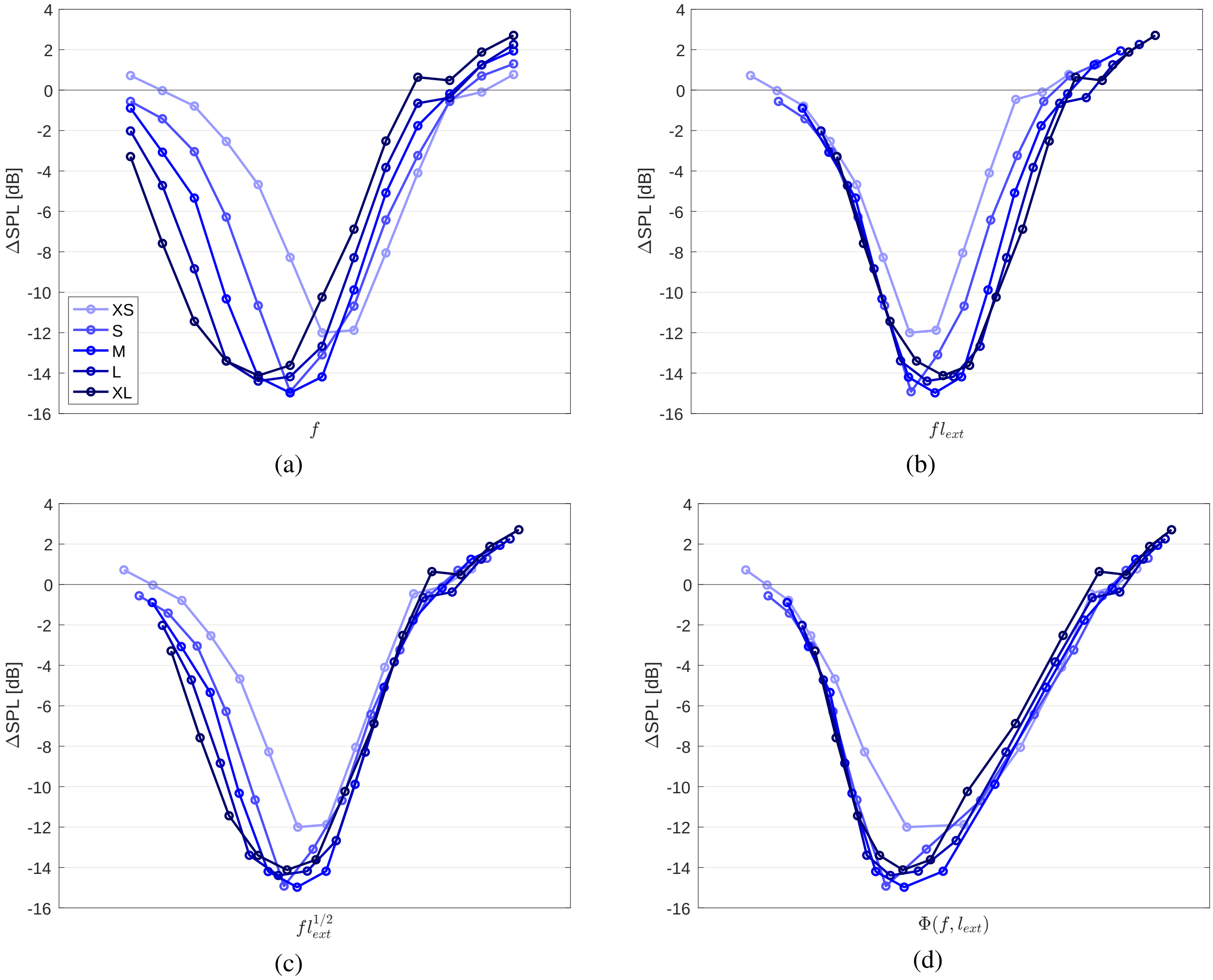

Figure 7 Noise reduction for different extension lengths at $U_\infty = 80$ m/s and $\alpha = 8°$. (a) Unscaled (b) Scaled for collapse at lower frequencies. (c) Scaled for collapse at higher frequencies. (d) Unified scaling.

$$\frac{\delta^*}{x} \approx \frac{1.83}{Re_x^{1/2}} \rightarrow \delta^* \approx 1.83x \left(\frac{\nu}{Ux}\right)^{1/2} \rightarrow \Delta\delta^* \propto \Delta x^{1/2} \quad (1)$$

$$f_{TBL-TE} \propto (\delta^*)^{-1} \rightarrow \Delta f \propto \Delta x^{-1/2} \rightarrow f l_{ext}^{1/2} \approx \text{Constant} \quad (2)$$

The two scaling behaviors can be combined into a unified function, $\Phi(f, l_{ext})$, as shown in Figure 7d. A good collapse is obtained across both frequency regimes, with the largest deviations occurring near the center of the noise reduction bucket. This is attributed to two factors: first, the center region represents a blend of the two distinct scaling mechanisms; second, the absolute sound levels are lowest in this region, leading to relatively higher measurement uncertainty. Furthermore, deviations are most pronounced for the shortest design (XS). This can already be seen in the unscaled curve, where its point of maximum noise reduction $(f_{peak}, \Delta\text{SPL}_{peak})$ diverges from the general trend of $(f_{peak}, \Delta\text{SPL}_{peak})$ with l_{ext}. This suggests that the proposed scaling laws are generally accurate for effective add-ons above a certain threshold l_{ext} and that the tested range in this study satisfied this criterion for all but the shortest design. The findings from this this analysis were verified for conditions (U_∞, α) outside the target design point as well. Overall, these scaling laws provide a practical framework for tailoring permeable extension designs to specific blade geometries and operational conditions, allowing optimization based on the characteristics of the relevant noise spectra.

4. Conclusion

This work presents the first publicly available full-scale acoustic measurements of permeable trailing-edge extensions for wind turbine blades. Testing was conducted under operationally relevant conditions in the Poul la Cour Tunnel (PLCT), using add-ons designed for standardised industry-grade production methods and materials while maintaining aerodynamic efficiency. Compared to the current status quo in serrations, the permeable extensions demonstrated an additional noise reduction of up to 3 dB(A) in overall sound pressure levels, with a maximum reduction of 8 dB(A) relative to an untreated blade.

The results confirm that permeable extensions not only maintain their noise reduction performance at full-scale conditions but benefit from scaling effects associated with increased blade chord and higher flow velocities. The extensions provided robust broadband reductions across a wide range of angles of attack, particularly at low-to-medium frequencies which typically cause the most problems as they travel furthest through the atmosphere. Secondary effects such as potential quasi-tonal, vortex shedding related humps, can be effective controlled with targeted design strategies. Additionally, we introduced scaling laws for a key design parameter — extension length — linking the frequency-dependent noise-reducing characteristics to the underlying physical mechanisms. These results offer a practical framework for tailoring permeable trailing-edge designs to different blade geometries and operational regimes.

Overall, the findings represent a significant step toward translating permeable trailing-edge extensions from laboratory concepts into commercially viable solutions. By combining validated robust acoustic performance and clear emperical scaling laws, permeable extensions offer a highly promising path forward for reducing wind turbine noise and enabling broader acceptance and further adoption of onshore wind energy.

Acknowledgments

This work is part of the Blade Extensions for Silent Turbines (BEST) project (HER+22-02-03415120) which is supported by the Netherlands Enterprise Agency (Rijksdienst voor Ondernemend Nederland (RVO)), acting on behalf of the Dutch Ministry of Economic Affairs, using the Renewable Energy Transition subsidy (subsidie Hernieuwbare Energietransitie (HER+ 2022-02)), part of the Topsector Energy (TSE) subsidies.

The authors gratefully acknowledge the staff of the Poul la Cour Tunnel for their support throughout the preparation, execution, and follow-up of the experimental campaign. We also thank Professor Chong (Brunel University) for his support in making the DRooTES model available for this study.

References

[1] S. Oerlemans, P. Sijtsma, and B. Méndez López, "Location and quantification of noise sources on a wind turbine," *Journal of Sound and Vibration*, vol. 299, no. 4, pp. 869–883, 2007.

[2] S. Oerlemans, M. Fisher, T. Maeder, and K. Kögler, "Reduction of wind turbine noise using optimized airfoils and trailing-edge serrations," *AIAA journal*, vol. 47, no. 6, pp. 1470–1481, 2009.

[3] F. Avallone, W. Van Der Velden, D. Ragni, and D. Casalino, "Noise reduction mechanisms of sawtooth and combed-sawtooth trailing-edge serrations," *Journal of Fluid Mechanics*, vol. 848, pp. 560–591, 2018.

[4] S. Oerlemans, "Wind turbine noise mitigation," in *Handbook of Wind Energy Aerodynamics*, pp. 1–16, Springer, 2021.

[5] T. Geyer, E. Sarradj, and C. Fritzsche, "Measurement of the noise generation at the trailing edge of porous airfoils," *Experiments in fluids*, vol. 48, pp. 291–308, 2010.

[6] T. Geyer, E. Sarradj, and C. Fritzsche, "Porous airfoils: noise reduction and boundary layer effects," *International journal of aeroacoustics*, vol. 9, no. 6, pp. 787–820, 2010.

[7] M. Herr, K.-S. Rossignol, J. Delfs, N. Lippitz, and M. Mößner, "Specification of porous materials for low-noise trailing-edge applications," in *20th AIAA/CEAS aeroacoustics conference*, p. 3041, 2014.

[8] A. Rubio Carpio, R. M. Martínez, F. Avallone, D. Ragni, M. Snellen, and S. van der Zwaag, "Experimental characterization of the turbulent boundary layer over a porous trailing edge for noise abatement," *Journal of Sound and Vibration*, vol. 443, pp. 537–558, 2019.

[9] A. Rubio Carpio, F. Avallone, D. Ragni, M. Snellen, and S. van der Zwaag, "3D-printed perforated trailing edges for broadband noise abatement," in *25th AIAA/CEAS aeroacoustics conference*, p. 2458, 2019.

[10] A. Rubio Carpio, F. Avallone, D. Ragni, M. Snellen, and S. van der Zwaag, "Quantitative criteria to design optimal permeable trailing edges for noise abatement," *Journal of Sound and Vibration*, vol. 485, p. 115596, 2020.

[11] S. Luesutthiviboon, D. Ragni, F. Avallone, and M. Snellen, "An alternative permeable topology design space for trailing-edge noise attenuation," *International Journal of Aeroacoustics*, vol. 20, no. 3-4, pp. 221–253, 2021.

[12] C. Teruna, F. Manegar, F. Avallone, D. Ragni, D. Casalino, and T. Carolus, "Noise reduction mechanisms of an open-cell metal-foam trailing edge," *Journal of Fluid Mechanics*, vol. 898, p. A18, 2020.

[13] C. Teruna, F. Avallone, D. Ragni, A. Rubio-Carpio, and D. Casalino, "Numerical analysis of a 3-D printed porous trailing edge for broadband noise reduction," *Journal of Fluid Mechanics*, vol. 926, p. A17, 2021.

[14] C. Jiang, D. Moreau, J. Fischer, and C. Doolan, "Additively manufactured sound-absorbing porous structures for airfoil trailing-edge noise control," *Journal of Aerospace Engineering*, vol. 34, no. 5, p. 04021068, 2021.

[15] C. Jiang, D. Moreau, C. de Silva, and C. Doolan, "Noise generation mechanisms of a micro-tube porous trailing edge," *Journal of Sound and Vibration*, vol. 571, p. 118085, 2024.

[16] M. Zhang and T. P. Chong, "Experimental investigation of the impact of porous parameters on trailing-edge noise," *Journal of Sound and Vibration*, vol. 489, p. 115694, 2020.

[17] C. Bak, A. S. Olsen, A. Fischer, O. Lylloff, R. Mikkelsen, M. Gaunaa, J. Beckerlee, S. Ildvedsen, T. Vronsky, F. Grasso, *et al.*, "Wind tunnel benchmark tests of airfoils," in *Journal of Physics: Conference Series*, vol. 2265, p. 022097, IOP Publishing, 2022.

[18] F. Bertagnolio, N. N. Sørensen, J. Johansen, and P. Fuglsang, "Wind turbine airfoil catalogue," 2001.

[19] M. Drela, "Xfoil: An analysis and design system for low reynolds number airfoils," in *Low Reynolds Number Aerodynamics: Proceedings of the Conference Notre Dame, Indiana, USA, 5–7 June 1989*, pp. 1–12, Springer, 1989.

[20] P. C. Woodhead, T. P. Chong, P. Joseph, and J. Wissink, "On the double-rooted trailing edge serration," in *25th AIAA/CEAS Aeroacoustics Conference*, p. 2436, 2019.

[21] A. Fischer, C. Bak, O. Lylloff, A. S. Olsen, R. F. Mikkelsen, S. B. Ildvedsen, J. S. Beckerlee, A. Borgoltz, M. Kuester, and N. Intaratep, "Cross validation of the aerodynamic and acoustic measurements in two Kevlar-walled wind tunnels," in *Journal of Physics: Conference Series*, vol. 2265, p. 022103, IOP Publishing, 2022.

[22] "Wind turbines – part 11: Acoustic noise measurement techniques," 2012. IEC 61400-11:2012.

[23] R. K. Amiet, "Noise due to turbulent flow past a trailing edge," *Journal of sound and vibration*, vol. 47, no. 3, pp. 387–393, 1976.

[24] H. Y. Hafeez and C. E. Ndikilar, "4 - boundary layer equations in fluid dynamics," in *Applications of Heat, Mass and Fluid Boundary Layers* (R. Fagbenle, O. Amoo, S. Aliu, and A. Falana, eds.), Woodhead Publishing Series in Energy, pp. 67–94, Woodhead Publishing, 2020.